Published online 15 June 2016

Nucleic Acids Research, 2016, Vol. 44, No. 13 ***6309–6317***
doi: 10.1093/nar/gkw539

Identification of a region in the coiled-coil domain of Smc3 that is essential for cohesin activity

Ola Orgil, Hadar Mor, Avi Matityahu and Itay Onn*

Faculty of Medicine in The Galilee, Bar-Ilan University, 8 Henrietta Szold Street, P.O. Box 1589, Safed 1311502, Israel

Received December 17, 2015; Revised May 30, 2016; Accepted June 3, 2016

ABSTRACT

The cohesin complex plays an important role in sister chromatin cohesion. Cohesin's core is composed of two structural maintenance of chromosome (SMC) proteins, called Smc1 and Smc3. SMC proteins are built from a globular hinge domain, a rod-shaped domain composed of long anti-parallel coiled-coil (CC), and a second globular adenosine triphosphatase domain called the head. The functions of both head and hinge domains have been studied extensively, yet the function of the CC region remains elusive. We identified a mutation in the CC of smc3 (L217P) that disrupts the function of the protein. Cells carrying the *smc3*-L217P allele have a strong cohesion defect and complexes containing smc3-L217P are not loaded onto the chromosomes. However, the mutation does not affect inter-protein interactions in either the core complex or with the Scc2 loader. We show by molecular dynamics and biochemistry that wild-type Smc3 can adopt distinct conformations, and that adenosine triphosphate (ATP) induces the conformational change. The L217P mutation restricts the ability of the mutated protein to switch between the conformations. We suggest that the function of the CC is to transfer ATP binding/hydrolysis signals between the head and the hinge domains. The results provide a new insight into the mechanism of cohesin activity.

INTRODUCTION

The four subunit cohesin complex mediates the formation of higher order chromatin structures by tethering two distinct regions of chromatin, either within the same DNA molecule, or between two distinct molecules (1). These functions are essential for the fidelity of chromosome segregation and condensation, DNA repair and regulation of gene expression (2–6).

The cohesin's core is formed by hetero-dimerization of two structural maintenance of chromosome (SMC) proteins called Smc1 and Smc3 (Figure 1A) (7). The SMC proteins are evolutionarily conserved in eukaryotes on both sequence and structure levels. They contain two globular domains called hinge and head domains, connected by a long coiled-coil (CC) domain. The head domain harbors two halves of an ABC-type adenosine triphosphatase (ATPase) domain (8). A ring-shaped trimer is formed by dimerization of two Smc hinges and adjoining the two Smc heads by interaction with adenosine triphosphate (ATP) and a third protein Mcd1/Scc1/Rad21 (7). Interaction of the cohesin subunit Mcd1 with the SMCs is mediated by the Smc1 head domain and the Smc3 neck domain (a break in the CC adjacent to the Smc3 head domain) (9–11). While the structural and functional activities of the hinge and the head domains were extensively studied, the function of the CC domain is poorly understood and its contribution to the molecular mechanism of cohesin activity is undetermined.

The CC domain may serve as an inert linker between the SMC functional domains or alternatively, it may have functional importance. One possible function of the CC might be to serve as a binding site of auxiliary proteins. *In vitro* screening, for peptides that interact with the cohesin loading protein Scc2, identified several regions of the SMC CC domain that may be involved in this interaction (12). Moreover, another member of the SMC family, Smc5 binds an important regulator, called Mms21, through its CC domain (13). However, to this date, no inter-molecular interaction other than the interaction with Mcd1 has been assigned to cohesin's CC domain. A second function of the CC may involve transferring signals from the head to the hinge. It has been suggested that crosstalk between head and hinge domains is a fundamental property of cohesin activity. ATP binding and hydrolysis in the head domain induces hinge opening and DNA binding. Therefore, the ATP binding/hydrolysis state of the head needs to be transferred to the hinge domain (14,15). However, elucidating the mechanism of this interaction remains a challenge.

Isolated cohesin complexes were observed by electron microscopy as rings (16). However, recent studies of bacterial SMC complexes by mass-spectrometry/cross-linking method identified inter-coiled coil interactions between the two SMC proteins (17). It has been revealed that the coiled coils of cohesin's Smc1 and Smc3 interact in a similar way (17). The model emerged from these studies suggest that

*To whom correspondence should be addressed. Tel: +972 72 2644 983; Fax: +972 72 2644 983; Email: Itay.Onn@biu.ac.il

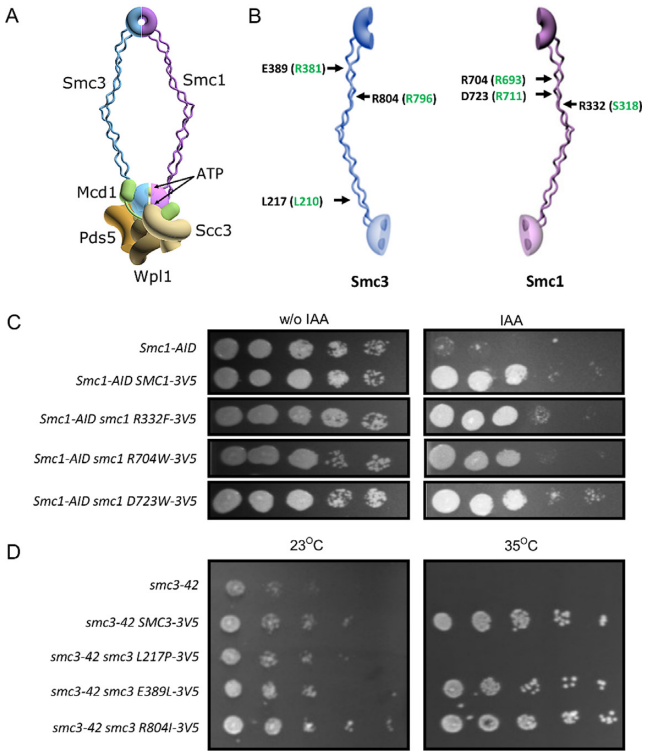

Figure 1. Identification of somatic mutations in the coiled-coil of Smc1 and Smc3. (**A**) Schematic presentation of the cohesin complex. The yellow balls between Smc1 and Smc3 represent ATP molecules. (**B**) Schematic presentation of Smc3 (blue) and Smc1 (purple) proteins; locations of chosen mutations are shown in yeast (black) and humans (green). (**C**) Strain YHG20 (SMC1-AID), carrying an ectopic copy of SMC1-3V5 (YHG-026), smc1-R332F-3V5 (YAM077), smc1-R704W-3V5 (YAM079) or smc1-D723W-3V5 (YAM080) were grown to saturation. Ten-fold serial dilutions of the strains were plated on plates with or without 1 mM IAA. (**D**) Strain YOG3064 (smc3-42), YOG3011 (SMC3-3V5 smc3-42), YOG3012 (smc3-L217P-3V5 smc3-42), YOG3013 (smc3-E389L-3V5 smc3-42) or YOG3014 (smc3-R804I-3V5 smc3-42) was grown to saturation. Ten-fold serial dilutions of the cells were plated and grown at either permissive (23°C) or restrictive (35°C) temperature.

cohesin alternates between an open and closed conformations. On the basis of this model we predicted that a mutant that cannot switch between conformations will not be active. However, such mutant has not been reported.

In recent years, cohesin has been identified as a central factor in human health. Mutations in genes encoding cohesin subunits and regulatory factors were identified in developmental disorders and tumorigenesis (18). Cornelia de Lange Syndrome (CdLS) is a genetic disorder that is associated with mutations in genes encoding for cohesin subunits. Of clinical cases defined as CdLS, about 5% and 1–2% of the cases are associated with a mutation in *SMC1A* or *SMC3*, respectively (19,20). In addition to developmental disorders, genomic analyses of tumors revealed that mutations in both *SMC1A* and *SMC3* are associated with cancer development (18). However, this type of analysis does not distinguish between driver and passenger mutations. When the mutation is located within a domain with an assigned function the phenotypic outcome of the mutation can be predicted to some extent. However, foreseeing the effect of a mutation that is not localized in a known functional domain is complicated. Furthermore, predicting the clinical significance of a mutation from the genomics of a tumor is a major challenge.

In this study, we surveyed *SMC1A* and *SMC3* cancer-related mutations in the Catalogue of Somatic Mutations in Cancer (COSMIC) database and classified these mutations based on their location in the SMC proteins. We identified a large number of mutations in the CC region of both Smc1 and Smc3. To assess the biological significance of some of these mutations we introduced them to the yeast Smc1 and Smc3 CC domains and characterized the effect of these mutant alleles on cohesin's function. We identified a missense mutation in the region of the kink domain of Smc3, which was previously identified in kidney carcinoma. The mutant allele does not support cohesion and the encoded protein does not bind to chromosomes. We show that the mutation induces a conformational change in Smc3 that presumably disconnects the transformation of signals between the head and the hinge domains. Analyzing this mutant provides an important insight into the molecular mechanism of cohesin activity.

MATERIALS AND METHODS

Yeast strains and media

Yeast strains and plasmids used in this study are listed in Supplementary Table S1 in the Supplementary Data. Yeast strains were grown in SC–LEU or YPD media supplemented with 2% glucose (21).

Site directed mutagenesis

Site-directed mutagenesis was performed on pVG451 (SMC1 T967-3V5, LEU2) and pVG428 (SMC3 V966-3V5, LEU2) using QuikChange II XL Site-Directed Mutagenesis Kit (Agilent) following the manufacturer's instructions. Primers used for the reactions are listed in Supplementary Table S2. pVG428 was a generous gift from Vincent Gucci and is related to the previously reported pVG393 and pVG395 (22,23). Detailed information regarding this plasmid is available upon request.

Cell synchronization

Cells were arrested in G1 phase by the addition of α-factor (1.5×10^{-8}M final). To release cells from α-factor-induced G1 arrest, cells were washed twice with media containing pronase E (0.1 mg/ml; Sigma) and twice in media without pronase E. Exponentially grown cultures were arrested in early S or G2/M using hydroxyurea (HU) (0.2 M) or nocodazole (NZ) (15 μg/ml final), respectively.

Cycloheximide chase analysis of protein stability

Cycloheximide (CHX) was added to mid-log phase cells at a final concentration of 35 μg/ml. Cell aliquots were taken hourly, washed and freeze in liquid nitrogen. To prepare cell lysates, cells were re-suspended in 200 μl 2% sodium dodecylsulphate (SDS) and were lysed by adding glass beads (Sigma) followed by four working cycles of 1 min in a bullet blender (Next Advance). The lysates were cleared

by two centrifugations of 5 and 15 min at 15 000 *g* at 4°C. Proteins were separated by sodium dodecyl sulphate-polyacrylamide gel electrophoresis (SDS-PAGE) and were analyzed by western blot with the indicated antibodies.

Whole cell extract fractionation

Cells were grown to mid-log phase. Whole cell extract and fractionation has been done as described in (24).

Immunoprecipitation and western blotting analysis

Cells were grown to mid-log phase, pelleted and washed with dH_2O and frozen in liquid nitrogen. Pellets were re-suspended in 350 μl IPH50 buffer (50 mM Tris, pH 8.0, 150 mm NaCl, 5 mM ethylenediaminetetraacetic acid, 0.5% NP-40, 1 mM β-mercaptoethanol, protease inhibitors cocktail (Sigma)). Cells were lysed by adding glass beads (Sigma) to the re-suspended pellets, followed by four working cycles of 1 min in a bullet blender (Next Advance). The lysate was cleared by two centrifugations of 5 and 15 min at 15 000 *g* at 4°C. Immunoprecipitations were performed at 4°C, after adding the appropriate antibodies for 2 h. The antibodies were collected on protein A/G agarose (Santa Cruz) or protein A magnetic beads (BioRAd) for 1 h and washed three times with IPH50 and resuspended in 35 μl Laemmli buffer. Standard procedures for SDS-PAGE, transferring proteins from to PVDF membrane (Millipore). Western blotting was performed by using SuperSignal West Pico (Thermo) and signals were detected by LAS 4000 (GE). The antibodies used in this study were: anti-HA (12CA5, Roche), anti-MYC (9E10, Roche), anti-V5 (Invitrogen/Millipore), Rabbit anti-Mcd1 (Rb555, provided by Vincent Guacci), Goat anti-Cdc4 (Santa Cruz Biotechnology), Rat monoclonal anti-Tubulin (Abcam) or Rabbit anti-histone H3 (Cell Signaling).

Cohesion spot assay

Cohesion at *LYS4* was assayed using the standard green fluorescent protein (GFP) assay. Cells were treated as described in the text and processed to visualize GFP foci by microscopy, as described previously (25). Each experiment was repeated three times and at least 300 cells were counted for each time-point in each experimental condition. Wide-field fluorescence images were obtained using the Zeiss AxioImager M2 fully motorized inverted microscope (100 X Plan-Apo, 1.4NA) fitted with an AxioCamHRm CCD High Resolution Camera.

Chromatin immunoprecipitation (ChIP)

Chromatin immunoprecipitation (ChIP) was performed as described (25).

Limited proteolysis

Immunoprecipitated Smc3-3V5, either wild-type or L217P, were incubated in 20 μl of buffer (50 mM Tris–HCl (pH 8.0) and 1 mM $MgCl_2$) with 5 mg/ml V8 protease (Worthington Biochemical), with or without 1 mM ATP (Sigma). The reaction was stopped at various time points by adding 20 μl of SDS sample buffer. Each reaction was loaded onto a SDS-gel and analyzed by western blot, using V5 antibody (Invitrogen/Millipore).

RESULTS

Identification of cancer-related mutations in the CC region of *SMC1A* and *SMC3*

We searched COSMIC (catalog of somatic mutations in a cancer) database for missense mutations in the cohesin subunits *SMC1A* and *SMC3* (Supplementary Table S3) (26,27). We counted 127 missense mutations in *SMC1A* and 118 missense mutations in *SMC3*. Of these mutations, 70% and 54% were located in the CC regions of SMC1A and SMC3, respectively. We expected that if these mutations are drivers they are in regions of functional importance. Based on this hypothesis we predicted that functional importance could be detected by evolutionary conservation of the residues. We explored this possibility using multiple sequence alignment, to identify the evolutionary conservation of the cancer-related mutated residue in the CC domains, between human and yeast Smc1 and Smc3. From this analysis we chose for further study six conserved residues that are located in the CC domains of Smc1 and Smc3 (Figure 1B and Supplementary Figure S1). The yeast Smc1 mutations R332F, R704W and D723W (S318F, R693W and R711W in humans) are located in the middle of the CC domain, toward the hinge. The yeast Smc3 mutations are L217P, E389L and R804I (L210P, R381L and R796I in humans). L217 is located at the region of the kink domain near the head, while E389 and R804 are closer to the hinge.

smc3-L217P-3V5 inhibits cell growth

To test the effect of *smc1* mutant alleles we constructed a strain in which Smc1 was fused to auxin induced degron (AID). The AID does not affect Smc1 functionality, as demonstrated by a cell growth assay (Supplementary Figure S2A). Western blot analysis of extracts from cells treated with 1 mM auxin showed complete depletion of the Smc1-AID-6Flag after 1 h (Supplementary Figure S2B). To test the ability of Smc1 CC mutants to support cell viability, we integrated *SMC1-3V5*, *smc1-R332F-3V5*, *smc1-R704W-3V5* or *smc1-D723W-3V5* into the *URA3* locus in the background of Smc1-AID-6Flag (strain yHG020). Cells were grown to saturation, serially diluted and spotted on plates with or without 1 mM IAA and grown at 30°C. The parent strain containing only *SMC1*-AID-6Flag allele did not grow while the addition of an ectopic copy of wild-type *SMC1* restored cell viability. No effect on growth was observed in strains that contained *smc1-R332F-3V5*, *smc1-R704W-3V5* or *smc1-D723W-3V5* when plates were supplemented with auxin to deplete Smc1-AID-6Flag. We concluded that the mutations in Smc1 CC do not interfere with the functionality of Smc1 and cohesin (Figure 1C).

Next, the effects of the mutations in Smc3 CC were explored. *SMC3-3V5*, *smc3-L217P-3V5*, *smc3-E389L-3V5* or *smc3-R804I-3V5* were integrated into *LEU2* in strain YIO141, which carried the *smc3-42* thermo-sensitive (ts) allele. As described above, cells were grown to saturation, se-

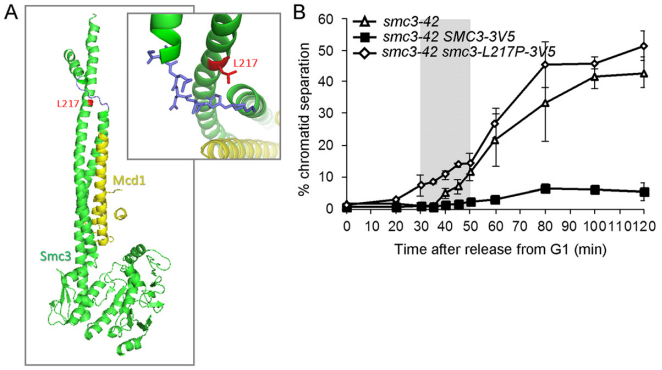

Figure 2. smc3-L217P does not support sister chromatid cohesion. (**A**) Crystal structure of *Saccharomyces cerevisiae* Smc3 (PDB ID: 4UX3). Marked in Green is Smc3 head and neck domains, marked in yellow is Mcd1. L217 residue is marked in red. The small picture depicts enlargement of the kink region (blue). (**B**) Strains YIO141 (smc3-42), YOG3011 (SMC3 smc3-42) and YOG3012 (smc3-L217P smc3-42) were grown at 23°C to mid-log phase and arrested in G1 using α-factor. Cells were shifted to 35°C for 1 h, released into the cell cycle and re-arrested in G2/M with nocodazole. Samples for cohesion assay were taken every 5-10 min. The gray frame indicates S-phase of the cell cycle as determined by flow cytometry (Supplementary Figure S3).

rially diluted and spotted on plates. Cells were incubated at either permissive (23°C) or restrictive (35°C) temperatures. All strains grew equally well at the permissive temperature. At 35°C, the *smc3-42* strain did not grow, while the ectopic wild-type *SMC3* allele rescued the cells, as expected. Two of the tested alleles, *smc3-E389L-3V5* and *smc3-R804I-3V5*, were viable at the restrictive temperature, suggesting that the mutated Smc3 proteins is active. However, cells carrying the *smc3-L217P-3V5* allele were unable to grow at the restrictive temperature. To exclude the possibility that the L217P mutation in Smc3 affects the stability of the protein we compared the stability of the wild-type and mutant proteins in cells. No difference in the stability of the wild-type and mutant protein was found (Supplementary Figure S3A). In addition, we tested the possibility that the mutation affects the nuclear localization of the mutant protein. We fractionated whole cell extract to cytoplasm and nucleoplasm and studied the localization of marker proteins, as well as Smc3 and Smc3 L217P (Supplementary Figure S3B). As expected, tubulin and histone H3 were enriched in the cytoplasmic and nucleoplasm fractions, respectively. Both the wild-type and the mutant Smc3 proteins were indistinguishably distributed between the fractions, suggesting that the L217P mutations do not affect the cellular localization of the protein. Therefore, our results indicate that the smc3-L217P is not functional (Figure 1D).

smc3-L217P-3V5 does not support sister chromatid cohesion

Residue L217 is located in the CC-46 amino acids from the head domain, opposite to a short break in the CC called the kink domain (Figure 2A) (11). To dissect the mechanism of smc3-L217P inactivation, we analyzed the molecular properties and activities of the protein. First, we tested whether cells are defective in sister chromatid cohesion. Cohesion was assessed using the standard GFP assay ('Materials and Methods' section). *smc3-42* cells alone (YIO141), or with an additional copy of *SMC3-3V5* (YOG3011) or *smc3-L217P-3V5* (YOG3012), were grown at the permissive temperature and arrested at the G1 stage of the cell cycle. Cells were shifted to the restrictive temperature of 35°C to inactivate *smc3-42*, released into the cell cycle and re-arrested in G2/M, by using the microtubule depolymerization drug, nocodazole (NZ). Samples were taken at the specified time points, after releasing the cells from the G1 arrest and processed for cohesion analysis. The percentage of cells that lost their sister chromatid cohesion was calculated by the ratio of GFP dots representing cohesion or cohesion loss ('Materials and Methods' section). Under the experimental conditions there was no cell cycle delay in the mutant strain compared with the wild-type cells, as indicated by flow cytometry (Supplementary Figure S4). Only 5% of *smc3-42* cells carrying the wild-type copy of *SMC3-3V5* lost sister chromatid cohesion (Figure 2B). In contrast, in both *smc3-42* and *smc3-L217P-3V5 smc3-42*, a cohesion defect was observed. The cohesion loss in the presence of smc3-L217P was detected 20 min after the release from G1, together with the initiation of DNA replication. The cohesion loss in the mutant cells was increased to about 50%, when cells reached G2/M. Interestingly, the cohesion loss in cells carrying *smc3-L217P-3V5* was observed earlier than in *smc3-42* cells. This finding suggests that the mechanism of cohesion loss in *smc3-42* and *smc3-L217-3V5* may be different.

smc3-L217P-3V5 inhibits cohesin loading onto chromosomes

To gain insight into the mechanism of the cohesion loss, we examined whether cohesin binding to chromosomes is defective in *smc3-L217P-3V5 smc3-42* cells, using ChIP. Strains YOG3011 (*SMC3-3V5 smc3*-42) and YOG3012 (*smc3-L217P-3V5 smc3-42*) were arrested in the G2/M phase. Cohesin association with chromatin was tested at the centromere of chromosome IV and at two cohesin enriched regions on the chromosome III arm, called CARC2 and CARC1 (Figure 3A and B). smc3-L217P-3V5 was not detected on the chromatin in any of the three regions, suggesting that the mutant is unable to stably bind chromatin.

The failure of smc3-L217P to induce cohesion in S phase, and its binding defect, can be explained by two distinct mechanisms. Mutated cohesin either failed to load onto chromosomes or its binding is unstable. To distinguish between these possibilities we performed two experiments. First, we tested whether smc3-L217P-3V5 is acetylated. Smc3 acetylation by Eco1 is a key event in cohesion establishment. The acetylation occurs during the S phase and only on chromatin-bound cohesin. It is unknown if acetylation is restricted to the chromatin-bound Smc3 due to spatial regulation of Eco1 or to a special conformation adopted by chromatin-bound Smc3. We speculated that the L217P mutation might adopt a structure that will enhance acetylation of the unbound protein. However, we did not detect acetylated Smc3 when we immunoprecipitated the smc3-L217P-3V5 (Figure 3C). This result is similar to that of the wild-type protein, in that smc3-L217P was not acetylated in its soluble form. To test the possibility of unstable binding, we performed ChIP from cells arrested in early S phase

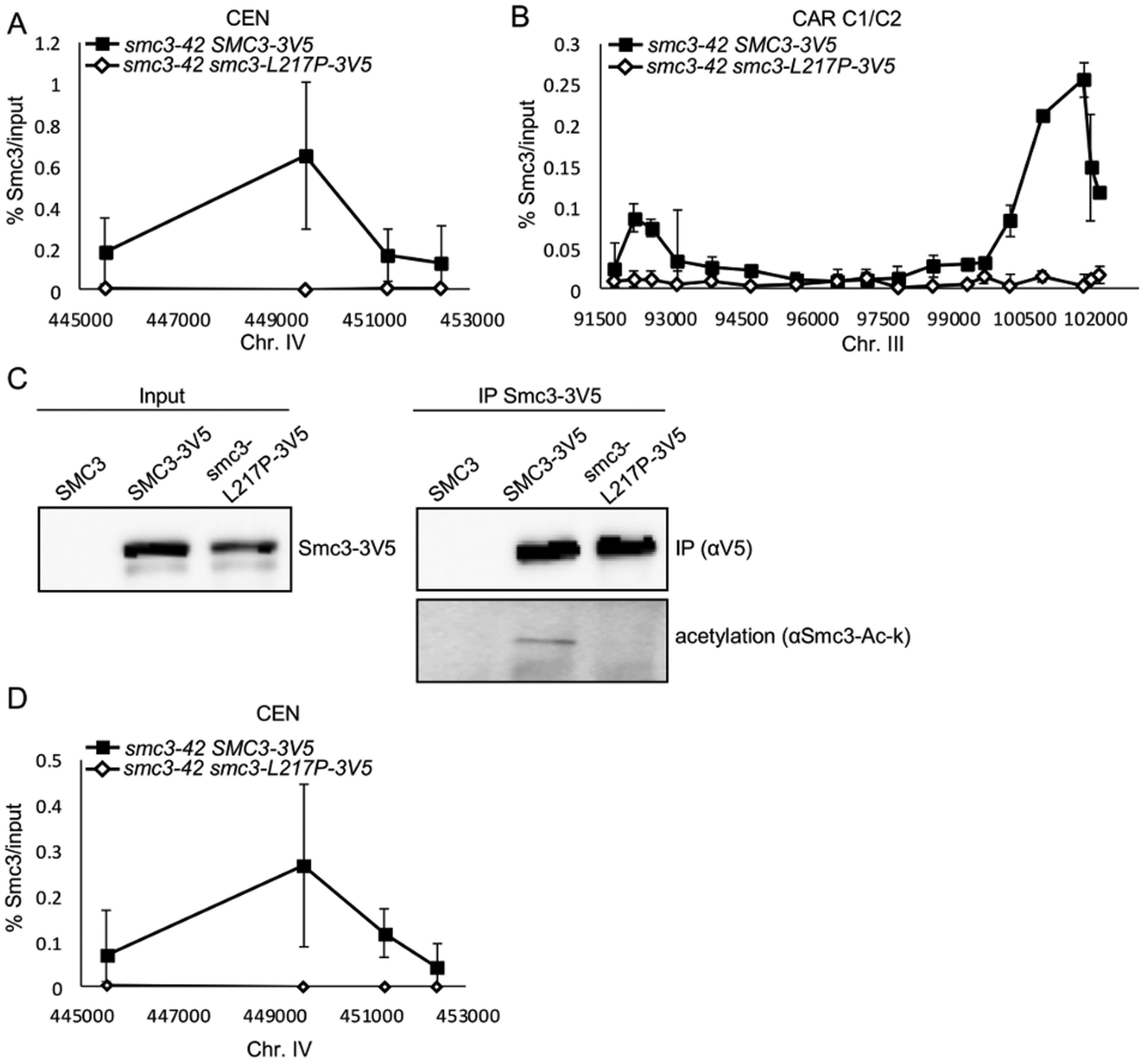

Figure 3. The smc3-L217P mutant does not bind chromosomes. YOG3011 (SMC3 smc3-42) and YOG3012 (smc3-L217P smc3-42) were arrested in G2/M and analyzed by a chromatin immunoprecipitation (ChIP) assay. An antibody against the V5 tag of either Smc3 or Smc3-L217P was used. Precipitated DNA was analyzed by quantitative PCR for CEN IV (**A**) and CARC2-CARC1 on chromosome III (**B**), as described ('Materials and Methods' section) ($n = 3$). (**C**) Strains YIO141 (smc3-42), YOG3011 (SMC3 smc3-42) and YOG3012 (smc3-L217P smc3-42) were grown to mid-log phase, lysed and subjected to immunoprecipitation against the V5 tag (Smc3). The acetylation state of the co-precipitated Smc3 was analyzed by western blot using antibodies against acetylated Smc3. (**D**) YOG3011 (SMC3 smc3-42) and YOG3012 (smc3-L217P smc3-42) were arrested in early S phase and processed for ChIP analysis. V5 tagged proteins were immunoprecipitated. Precipitated DNA was analyzed by quantitative PCR for CEN IV. ($n = 3$).

by hydroxyurea (HU). If cohesin is loaded at early S but is not detected at G2/M, it may imply on a deficiency in post-establishment cohesion maintenance. Cohesin binding was measured at the centromere of chromosome IV (Figure 3D). Since cells are arrested in early S phase, the cohesin enrichment signal is lower than G2/M phase arrested cells. However, smc3-L217P-3V5 was not detected on the chromosome, indicating that the binding defect is due to a loading rather than a cohesion maintenance problem.

smc3-L217P-3V5 does not affect the interaction with the cohesin loader and core cohesin subunits

Cohesin loading is mediated by the Scc2/4 loader. Since smc3-L217P fails to interact with chromatin we sought to explore the possibility that the L217P mutation affects the interaction with the loader. Scc2 was tagged with 12 copies of Myc epitope in strains carrying either Smc3-3V5 or smc3-L217P-3V5. We immunoprecipitated Smc3 with an antibody against V5 from these cells and analyzed the

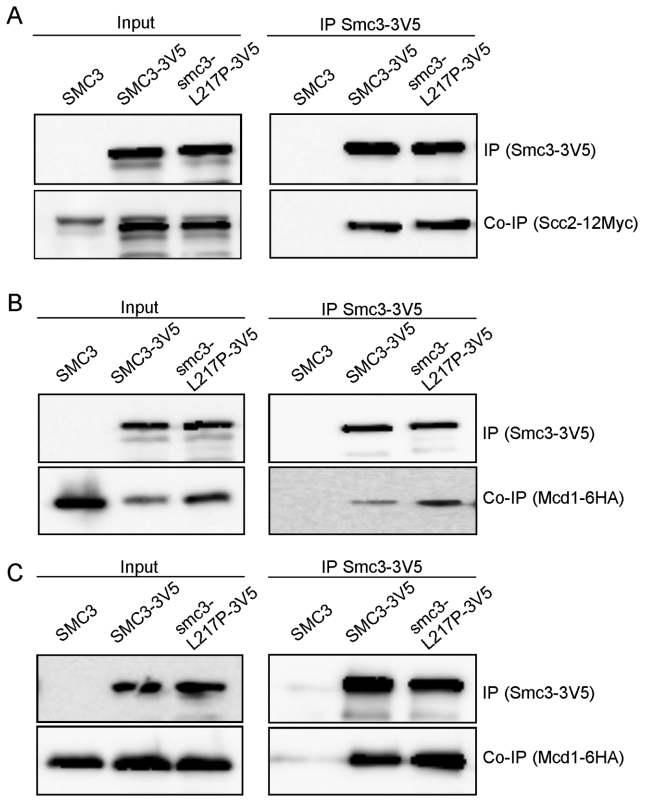

Figure 4. The smc3-L217P mutation does not affect binding to Scc2 nor binding to Scc3 or Mcd1. (**A**) Strains YMS1003 (SCC2-12MYC), YOG3031 (SCC2-12MYC SMC3-3V5) or YOG3032 (SCC2-12MYC smc3-L217P-3V5) were grown to mid-log phase. Cells were lysed and subjected to immunoprecipitation against the V5 tag (Smc3). The co-precipitation of Scc2 binding was analyzed by western blot using antibodies against Myc. (**B**) Strains Y5322 (SCC3-6HA), YOG3035 (SCC3-6HA SMC3-3V5) and YOG3036 (SCC3-6HA smc3-L217P-3V5) were prepared for IP as described in (A). Co-precipitated proteins were analyzed by western blot using antibodies against HA. (**C**) Strains YIO189 (MCD1-6HA), YOG3028 (MCD1-6HA SMC3-3V5) and YOG3029 (MCD1-6HA smc3-L217P-3V5) were prepared for IP as described in (A). Co-precipitated proteins were analyzed by western blot using antibodies against HA.

co-immunoprecipitation (co-IP) of Scc2-12Myc by western blot. The co-precipitation of Scc2 was similar when either the native or the mutant protein was pulled down (Figure 4A). These results suggest that the L217P mutation does not affect the interaction with the loader.

Smc3 is a core subunit of the cohesin ring. We therefore tested the possibility that the L217P mutation affects the cohesin complex assembly in a series of co-IPs. We tested the co-IP of Scc3-6HA with Smc3-3V5 or smc3-L217P-3V5. No difference in the co-IP levels of Scc3 were found when either the native or the mutant Smc3 was pulled down (Figure 4B). L217 is located about 10 amino-acids away from the neck-domain, Therefore, the L217P mutation may interfere with Mcd1 binding (11). Extracts were prepared from cells carrying Mcd1-6HA with untagged Smc3, Smc3-3V5 or smc3-L217P-3V5. The V5 tagged proteins were immunoprecipitated and the co-precipitation of Mcd1-6HA was detected (Figure 4C). However, no difference was found in the levels of Mcd1 bound to either the native or the mutant proteins.

Mcd1 is bound to both Smc3 and Smc1 (9). Therefore, the Co-IP of Mcd1 may look unaffected if the Smc3–Smc1 interaction is unperturbed. To exclude this possibility we used the yHG-020 (Smc1-AID-6Flag) strain bearing either wild-type Smc3-3V5 or smc3-L217P-3V5. The cells were grown to the mid-log phase. Smc1 was depleted *in vivo* by supplementing the medium with 1 mM IAA for 1 h. The levels of V5-tagged proteins in the extract were measured by western blot. As expected, the Smc1-AID-6Flag was depleted to undetectable levels after treatment with auxin. Unexpectedly, Mcd1 levels were also decreased to undetected levels and made the experiment unfeasible (Supplementary Figure S5). Interestingly, a similar decrease in Mcd1 levels was not observed in our previous work in which Scc3 was depleted (25). Under these conditions the experiment could not be performed.

The L217P mutation induces a conformational change in Smc3

Our experiments did not support a model in which the L217P mutation inhibits protein-protein interaction. Therefore, we sought to test the effect of the mutation on Smc3 conformation. Recent cross-linking/mass spectrometry experiments implied that the CC domains of SMC proteins shift between open and closed forms (28). We speculated that inserting proline into the coil may break the coil structure. We used a structural bioinformatics approach to test this hypothesis. The secondary structure of smc3-L217P was predicted by PSIPRED (29). Replacement of leucine 217 with proline broke the helical structure, as predicted (Supplementary Figure S6). To further explore the global effects of this mutation on the conformation of Smc3 we used the crystal structure of Smc3 (PDB ID: 4UX3) as a template to create a model of smc3-L217P in I-TASSER server (11,30). We analyzed the molecular dynamics of Smc3 and smc3-L217P by using the elNemo server (31). We examined the <R2> factor of both proteins, which represents their flexibility (Supplementary Figure S7). Low <R2> indicates rigidity, while a high <R2> value indicates flexibility of the molecule. The analysis revealed high flexibility of the wild-type protein, while the range of the movement was limited in smc3-L217P.

The conformational flexibility in the wild-type Smc3 may represent the unbound and ATP bound forms of the protein. Bioinformatics suggest that the L217P mutation breaks the CC and limits the switch between the conformations. We explored this possibility by limited proteolysis of Smc3. In this assay, the protein is incubated with a protease, allowing partial cleavage of the protein (32). The sensitivity of the cleavage sites depends on the conformation of the protein. A comparison of the obtained fragments between native protein and mutant proteins, with and without ATP, can indicate different conformations. The V8 protease cleaves peptide bonds C-terminal to glutamic acid was used for limited proteolysis. Smc3-3V5 or smc3-L217P-3V5 were precipitated from asynchronous cell cultures and incubated with V8 protease, with or without ATP. The reaction products were analyzed by western blot with antibodies against V5. Figure 5 shows that both the native and the mutant proteins have ∼170 kDa mass (a).

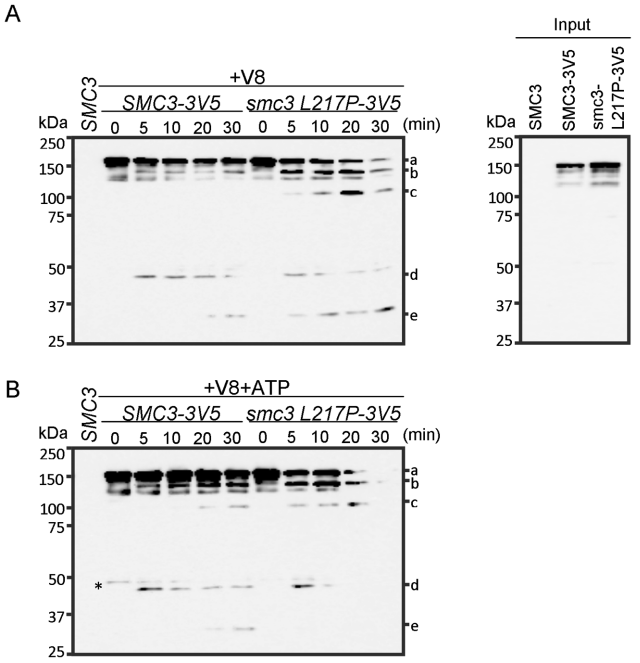

Figure 5. Proteolytic cleavage of Smc3 wild-type and mutant proteins. Smc3-V5 and smc3-L217P-3V5 were pulled down by using antibodies against V5. The precipitated proteins were washed and incubated with V8 protease at 23°C in the absence (**A**) or presence (**B**) of 1 mM ATP. The reactions were stopped at the indicated time points. The cleaved products were resolved by sodium dodecyl sulphate-polyacrylamide gel electrophoresis and analyzed by western blot, using antibody against V5. The major cleaved products discussed in the text are labeled as a–e. * indicates a non-specific band. A representative experiment is shown. ($n = 4$).

During incubation with the protease (Figure 5A), two proteolytic fragments of ∼140 kDa (b) and ∼45 kDa (d) were detected in the wild-type protein, after 5 min of incubation. After 15 more minutes, ∼45 kDa fragment (d) started to disappear and a new fragment of ∼30 kDa (e) started to accumulate. With striking difference, smc3-L217P was more sensitive to cleavage by the protease. In addition, a new fragment of ∼110 kDa (c) appeared after 5 min of incubation with the protease. Since we took advantage of an internally tagged protein, the molecular weight of the fragments is not indicative of the location of the cleavage site.

ATP has been suggested to be the driver of the conformational change in Smc3. To explore this possibility we repeated the limited proteolysis experiment after supplementing the reaction mixture with 1 mM ATP (Figure 5B). Addition of ATP to the wild-type protein induced the appearance of the ∼110 kDa (c) fragment, previously observed only in the smc3-L217P protein. In smc3-L217P, ATP accelerated the degradation of the 45 kDa (d) fragment; however, no accumulation of the ∼30 kDa (e) fragment was observed. These results support the model in which ATP induces a conformational change in Smc3 and cohesin, and suggest that the L217P mutation shifts Smc3 to the ATP-bound conformation.

A mutation in the helix complementary to L217 does not support cell viability

We sought to determine whether the functional importance of L217 is limited to this residue or defines a functional region in the protein. To explore these possibilities we introduced a mutation in the proximity of L217, in the corresponding helix. We selected a mutation from COSMIC that were previously identified in tumors. E987 (E975 in humans) is located in the spatial region of L217 but on the opposite helix (Supplementary Figure S8A). The negatively charged glutamic acid at position 987 was changed to a positively charged lysine (E987K) by site directed mutagenesis of SMC3-3V5 (Supplementary Figure S8A). Prediction of the secondary structure reveals that the mutation extends a natural occurring break in the coil. Therefore, E987K may be deleterious. The mutant genes were integrated at LEU2 in the background of *smc3-42*. The ability of smc3 E987-3V5 to support cell growth was determined by semi-quantitative growth assay at permissive (23°C) and restrictive (35°C) temperatures. The results show that in agreement with the predicted effect, smc3 E987-3V5 does not supported cell growth when smc3-42 was inactivated (Figure 6). The results suggest that this region in the coiled coil is important for the molecular activity of cohesin.

DISCUSSION

This study provides a new insight into the mechanism of Smc3 function through analysis of a mutation in its CC domain. We showed that smc3 L217P mutant protein induces cohesion loss during the cell cycle because the cohesin complexes fail to load onto the chromatin. However, the overall architecture of the mutant complex remains unaffected. The L217P mutation induces a conformational change in Smc3. We demonstrated that the CC region of Smc3 is critical for the conformational switch of Smc3. We also show that a mutation in other residues in this region E987K, which is located at the same region, is important for cell viability, most likely through the inactivation of cohesin. These results suggest that this region in the coiled coil of Smc3 plays a key role in the action mechanism of cohesin. Based on our findings, we suggest a working model. Smc3 alternates between conformation C and D. Conformation C is associated with loading while conformation D is related to cohesion (Figure 7). Switching from conformation C to D is a critical step in the cohesin activity cycle. Two main questions arise from this model. What induces the conformational change and what stabilizes the protein in the correct conformation?

What drives the conformational change of Smc3? One possibility is that the interaction with the Scc2/4 loader induces the conformational change. Our results show similar interaction between Scc2 and either Smc3 or smc3-L217P. Therefore, we conclude that the mutation does not inhibit the interaction. The second possibility is that Smc3 acetylation by Eco1 serves as an inducer of the conformational change (33,34). However, this possibility is unlikely since smc3-L217P is not acetylated. The third possibility is that ATP induces the conformational change and in turn induces the loading pro-forms of cohesin (12,22,35–37). Indeed, ATP has been shown to induce conformational changes in many proteins including the SMC-related ABC

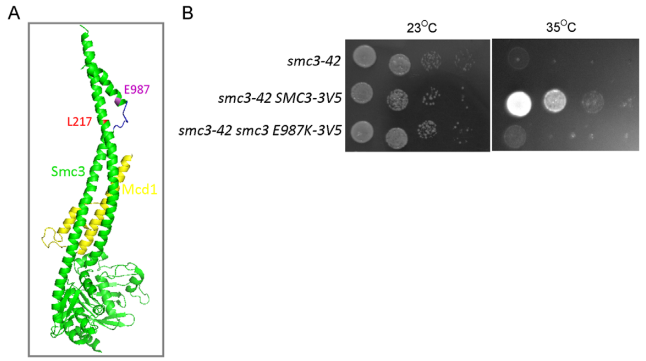

Figure 6. The L217 region is important for cohesin activity. (**A**) Crystal structure of *Saccharomyces cerevisiae* Smc3 (PDB ID: 4UX3). The head and neck domains of Smc3 are green. The kink domain is in blue and Mcd1 is in yellow. L217 and E987 are marked in magenta. (**B**) Strain YOG3064 (smc3-42), YOG3011 (SMC3-3V5 smc3-42), YOG3102 (smc3-E987K-3V5 smc3-42) was grown to saturation. Ten-fold serial dilutions of the cells were plated and grown at either permissive (23°C) or restrictive (35°C) temperature.

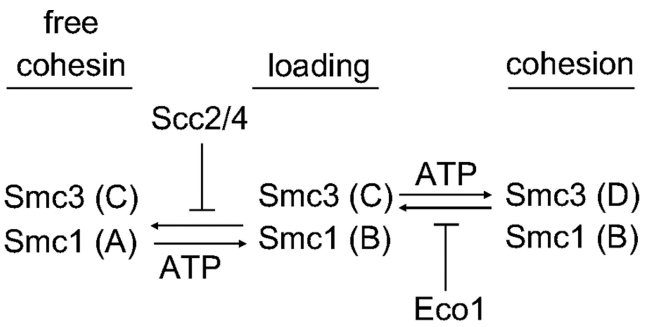

Figure 7. A model for cohesin mechanism of action. Smc1 and Smc3 alternate between two conformations (A-B and C-D, respectively). ATP binding/hydrolysis is the inducer of the conformational switches. The Scc2/4 loader stabilized the loading-pro B conformation of Smc1. Acetylation of Smc3 by Eco1 during S phase stabilizes Smc3 in the cohesive-pro D conformation.

transporters and in the condensin subunit SMC2 (32,38). In addition, recent dynamic analysis of Smc2-Smc4 dimer by high speed AFM revealed that the SMC dimer is very flexible (39). The limited proteolysis results we presented show an ATP binding-dependent conformational change in Smc3. We therefore prefer the third model in which ATP binding and hydrolysis induce the intra-molecular changes in Smc3.

The conformational change may be associated with one or more molecular activities. First, it may be associated with loading-related hinge opening (14). Dissociation of the Smc1 and Smc3 hinges has been suggested as a step in cohesin loading. We disfavor this model because recent reports showed that cohesin loading depends on the ATP binding activity of Smc1 but not of Smc3 (22). Therefore, we suggest that Scc2/4 stabilize a conformational change in Smc1 to allow loading. Smc3 ATPase activity has been suggested to be associated with tethering activity, which is independent of loading activity (22). In bacterial Smc3 proteins, ATPase hydrolysis has been shown to be required for DNA binding at the hinge (15). Based on this evidence we suggest that conformational changes in Smc1 and Smc3 are functionally distinct and are associated with loading and tethering, respectively.

Cross-linking mass-spectrometry analysis of bacterial SMCs and cohesin revealed open and closed conformations of the central ring (17,28). Based on these studies and the results we presented here we suggest the following model for cohesin mechanism of action (Figure 7). ATP induces a conformational change in Smc1, from A to B, which allows cohesin binding. We suggest that the role of Scc2/4 is to stabilize Smc1 in the B conformation. A post-loading ATP-dependent Smc3 conformational change transforms Smc3 from conformation C to conformation D. Acetylation of Smc3 by Eco1 stabilizes Smc3 in the cohesive D conformation. smc3-L217P is locked in the D conformation and cannot adopt the C conformation that allows loading.

An interesting finding of this work is that Mcd1 is unstable when Smc1 is depleted. Similar instability was not observed when Smc3 was depleted (25). This implies a fundamental difference between Smc1–Mcd1 and Smc3–Mcd1. If the interaction between Smc1 and Mcd1 is stable, the depletion of Smc1 exposes the N'-terminal of Mcd1 to proteolysis. The interface between Smc3 and Mcd1 has been suggested to be the exit gate of the DNA (14). In this case, the Smc3–Mcd1 interaction is dynamic and frequently results in the exposure of the Mcd1 C'-terminal. Therefore, our results support the exit gate model between Smc3–Mcd1.

Our initial observation of the smc3-L217P and E987K mutations were in the human tumor. In addition to cancer, 1–2% of the clinically defined cases of CdLS are associated with a mutation in Smc3 (20). Six CdLS-related mutations have been reported in the kink region: T235del, R236P, E287dup, R839C, L832_N833del and H917P. The inability of the mutants we tested in this study may suggest on a similar mechanism in cancer cells. Some of the mutants that have been studied here did not affect yeast cell viability. However, the possibility that these mutations are associated with other cohesin functions such as gene expression cannot be excluded. Therefore, their involvement in tumorigenesis cannot be ruled out.

The damaging mutations we identified are associated with breakage of the helix. We suggest that mutations in the kink domain in h*SMC3* that break the coil structure in this region are associated with human diseases. Therefore, structural bioinformatics that predict the effect of a mutation on helix conformation may be used in these cases to predict clinical outcome.

SUPPLEMENTARY DATA

Supplementary Data are available at NAR Online.

ACKNOWLEDGEMENT

We would like to thank the members of the Onn laboratory for their discussion and comments on the manuscript; Vincent Guacci for reagents; Yehuda Brody and Eyla Maoz for their technical help with imaging and cytometry.

FUNDING

Israel Cancer Association [ICA20130124]; Jerome Lejeune Foundation [1146-OI2013_A]; Leona M. and Harry B.

Helmsley Charitable Trust [2012PG-ISL013]. Funding for open access charge: Leona M. and Harry B. Helmsley Charitable Trust Research Grant [2012PG-ISL013].
Conflict of interest statement. None declared.

REFERENCES

1. Onn,I., Heidinger-Pauli,J.M., Guacci,V., Unal,E. and Koshland,D.E. (2008) Sister chromatid cohesion: a simple concept with a complex reality. *Annu. Rev. Cell Dev. Biol.*, **24**, 105–129.
2. Dorsett,D., Eissenberg,J.C., Misulovin,Z., Martens,A., Redding,B. and McKim,K. (2005) Effects of sister chromatid cohesion proteins on cut gene expression during wing development in Drosophila. *Development*, **132**, 4743–4753.
3. Guacci,V., Koshland,D. and Strunnikov,A. (1997) A direct link between sister chromatid cohesion and chromosome condensation revealed through the analysis of MCD1 in S. cerevisiae. *Cell*, **91**, 47–57.
4. Michaelis,C., Ciosk,R. and Nasmyth,K. (1997) Cohesins: chromosomal proteins that prevent premature separation of sister chromatids. *Cell*, **91**, 35–45.
5. Unal,E., Arbel-Eden,A., Sattler,U., Shroff,R., Lichten,M., Haber,J.E. and Koshland,D. (2004) DNA damage response pathway uses histone modification to assemble a double-strand break-specific cohesin domain. *Mol. Cell*, **16**, 991–1002.
6. Unal,E., Heidinger-Pauli,J.M. and Koshland,D. (2007) DNA double-strand breaks trigger genome-wide sister-chromatid cohesion through Eco1 (Ctf7). *Science*, **317**, 245–248.
7. Nasmyth,K. and Haering,C.H. (2009) Cohesin: its roles and mechanisms. *Annu. Rev. Genet.*, **43**, 525–558.
8. Hirano,T. (2005) SMC proteins and chromosome mechanics: from bacteria to humans. *Philos. Trans. R. Soc. Lond. B Biol. Sci.*, **360**, 507–514.
9. Haering,C.H., Lowe,J., Hochwagen,A. and Nasmyth,K. (2002) Molecular architecture of SMC proteins and the yeast cohesin complex. *Mol. Cell*, **9**, 773–788.
10. Haering,C.H., Schoffnegger,D., Nishino,T., Helmhart,W., Nasmyth,K. and Lowe,J. (2004) Structure and stability of cohesin's Smc1-kleisin interaction. *Mol. Cell*, **15**, 951–964.
11. Gligoris,T.G., Scheinost,J.C., Burmann,F., Petela,N., Chan,K.L., Uluocak,P., Beckouet,F., Gruber,S., Nasmyth,K. and Lowe,J. (2014) Closing the cohesin ring: structure and function of its Smc3-kleisin interface. *Science*, **346**, 963–967.
12. Murayama,Y. and Uhlmann,F. (2014) Biochemical reconstitution of topological DNA binding by the cohesin ring. *Nature*, **505**, 367–371.
13. Duan,X., Yang,Y., Chen,Y.H., Arenz,J., Rangi,G.K., Zhao,X. and Ye,H. (2009) Architecture of the Smc5/6 Complex of Saccharomyces cerevisiae Reveals a Unique Interaction between the Nse5-6 Subcomplex and the Hinge Regions of Smc5 and Smc6. *J. Biol. Chem.*, **284**, 8507–8515.
14. Gruber,S., Arumugam,P., Katou,Y., Kuglitsch,D., Helmhart,W., Shirahige,K. and Nasmyth,K. (2006) Evidence that loading of cohesin onto chromosomes involves opening of its SMC hinge. *Cell*, **127**, 523–537.
15. Hirano,M. and Hirano,T. (2006) Opening closed arms: long-distance activation of SMC ATPase by hinge-DNA interactions. *Mol. Cell*, **21**, 175–186.
16. Anderson,D.E., Losada,A., Erickson,H.P. and Hirano,T. (2002) Condensin and cohesin display different arm conformations with characteristic hinge angles. *J. Cell Biol.*, **156**, 419–424.
17. Burmann,F., Shin,H.C., Basquin,J., Soh,Y.M., Gimenez-Oya,V., Kim,Y.G., Oh,B.H. and Gruber,S. (2013) An asymmetric SMC-kleisin bridge in prokaryotic condensin. *Nat. Struct. Mol. Biol.* **20**, 371–379.
18. Mannini,L. and Musio,A. (2011) The dark side of cohesin: the carcinogenic point of view. *Mutat. Res.*, **728**, 81–87.
19. Mannini,L., Cucco,F., Quarantotti,V., Krantz,I.D. and Musio,A. (2013) Mutation spectrum and genotype-phenotype correlation in cornelia de lange syndrome. *Hum. Mutat.*, **34**, 1589–1596.
20. Gil-Rodriguez,M.C., Deardorff,M.A., Ansari,M., Tan,C.A., Parenti,I., Baquero-Montoya,C., Ousager,L.B., Puisac,B., Hernandez-Marcos,M., Teresa-Rodrigo,M.E. *et al.* (2015) De novo heterozygous mutations in SMC3 cause a range of Cornelia de Lange syndrome-overlapping phenotypes. *Hum. Mutat.*, **36**, 454–462.
21. Guthrie,C. and Fink,G.R.E. (1991) *Guide to Yeast Genetics and Molecular Biology*. Academic Press, NY.
22. Camdere,G., Guacci,V., Stricklin,J. and Koshland,D. (2015) The ATPases of cohesin interface with regulators to modulate cohesin-mediated DNA tethering. *Elife*, **4**, e11315.
23. Eng,T., Guacci,V. and Koshland,D. (2014) ROCC, a conserved region in cohesin's Mcd1 subunit, is essential for the proper regulation of the maintenance of cohesion and establishment of condensation. *Mol. Biol. Cell*, **25**, 2351–2364.
24. Liang,C. and Stillman,B. (1997) Persistent initiation of DNA replication and chromatin-bound MCM proteins during the cell cycle in cdc6 mutants. *Genes Dev.*, **11**, 3375–3386.
25. Orgil,O., Matityahu,A., Eng,T., Guacci,V., Koshland,D. and Onn,I. (2015) A conserved domain in the scc3 subunit of cohesin mediates the interaction with both mcd1 and the cohesin loader complex. *PLoS Genet.*, **11**, e1005036.
26. Forbes,S.A., Bindal,N., Bamford,S., Cole,C., Kok,C.Y., Beare,D., Jia,M., Shepherd,R., Leung,K., Menzies,A. *et al.* (2011) COSMIC: mining complete cancer genomes in the catalogue of somatic mutations in cancer. *Nucleic Acids Res.*, **39**, D945–D950.
27. Forbes,S.A., Bhamra,G., Bamford,S., Dawson,E., Kok,C., Clements,J., Menzies,A., Teague,J.W., Futreal,P.A. and Stratton,M.R. (2008) The catalogue of somatic mutations in cancer (COSMIC). *Curr. Protoc. Hum. Genet.*, **57**, 1–26.
28. Soh,Y.M., Burmann,F., Shin,H.C., Oda,T., Jin,K.S., Toseland,C.P., Kim,C., Lee,H., Kim,S.J., Kong,M.S. *et al.* (2015) Molecular basis for SMC rod formation and its dissolution upon DNA binding. *Mol. Cell*, **57**, 290–303.
29. Jones,D.T. (1999) Protein secondary structure prediction based on position-specific scoring matrices. *J. Mol. Biol.*, **292**, 195–202.
30. Zhang,Y. (2008) I-TASSER server for protein 3D structure prediction. *BMC Bioinformatics*, **9**, 40.
31. Suhre,K. and Sanejouand,Y.H. (2004) ElNemo: a normal mode web server for protein movement analysis and the generation of templates for molecular replacement. *Nucleic Acids Res.*, **32**, W610–W614.
32. Onn,I., Aono,N., Hirano,M. and Hirano,T. (2007) Reconstitution and subunit geometry of human condensin complexes. *EMBO J.*, **26**, 1024–1034.
33. Rolef Ben-Shahar,T., Heeger,S., Lehane,C., East,P., Flynn,H., Skehel,M. and Uhlmann,F. (2008) Eco1-dependent cohesin acetylation during establishment of sister chromatid cohesion. *Science*, **321**, 563–566.
34. Unal,E., Heidinger-Pauli,J.M., Kim,W., Guacci,V., Onn,I., Gygi,S.P. and Koshland,D.E. (2008) A molecular determinant for the establishment of sister chromatid cohesion. *Science*, **321**, 566–569.
35. Arumugam,P., Gruber,S., Tanaka,K., Haering,C.H., Mechtler,K. and Nasmyth,K. (2003) ATP hydrolysis is required for cohesin's association with chromosomes. *Curr. Biol.*, **13**, 1941–1953.
36. Heidinger-Pauli,J.M., Onn,I. and Koshland,D. (2010) Genetic evidence that the acetylation of the Smc3p subunit of cohesin modulates its ATP-bound state to promote cohesion establishment in Saccharomyces cerevisiae. *Genetics*, **185**, 1249–1256.
37. Hu,B., Itoh,T., Mishra,A., Katoh,Y., Chan,K.L., Upcher,W., Godlee,C., Roig,M.B., Shirahige,K. and Nasmyth,K. (2011) ATP hydrolysis is required for relocating cohesin from sites occupied by its Scc2/4 loading complex. *Curr. Biol.*, **21**, 12–24.
38. Wilkens,S. (2015) Structure and mechanism of ABC transporters. *F1000Prime Rep.*, **7**, 14.
39. Eeftens,J.M., Katan,A.J., Kschonsak,M., Hassler,M., de Wilde,L., Dief,E.M., Haering,C.H. and Dekker,C. (2016) Condensin Smc2-Smc4 dimers are flexible and dynamic. *Cell Rep.*, **14**, 1813–1818.